

Recomputing the Hubble constant

Joan Alcaide Núñez

December 20, 2023

ABSTRACT

The Hubble constant has been derived multiple times, however, it can not be agreed on a specific value. We recompute this value applying the same methods as Hubble did with more modern data. Making use of Cepheid variable stars as distance indicators and redshift for calculating radial velocities. We recover a value of $48.5 \pm 5.4 \text{ kms}^{-1} \text{ Mpc}^{-1}$ as the Hubble constant. We discuss the results and relate them to the Big Bang theory of an expanding Universe, its implications in mathematical proofs, and further cosmological calculations of the Hubble parameter and the deceleration constant. Finally, we compare our results with previous calculations and consider our value inconsistent with previous estimates.

1 INTRODUCTION

The Hubble constant represents the local expansion rate of the Universe, sets its overall scale, and enables the determination of its age and history, therefore, it is a fundamental measure in cosmology (Ryden 2017). This constant was first derived by the astronomers Georges Lemaître and Edwin Hubble, who discovered the relation between distance and radial velocity of "extra-galactic Nebulae", and computed a value of $k = 575 \text{ kms}^{-1} \text{ Mpc}^{-1}$ (Lemaître 1927) and $k = 513 \text{ kms}^{-1} \text{ Mpc}^{-1}$ (Hubble 1929), respectively¹. It was shown that those extra-galactic Nebulae are in fact other galaxies and that the majority of them are moving away. The Hubble law is expressed as follows:

$$v = H_0 d \quad (1)$$

Where v is the radial velocity, d is the distance and H_0 is the Hubble constant.

The observation of the proportionality between distance and radial velocity can be explained by the Big Bang model of the Universe, which states that this is caused by the expansion of the Universe and that the Hubble constant stand for the expansion rate (de Sitter 1930). In addition, this observation supports the Big Bang model rather than the Steady State model. This second theory states that the Universe has and will remain identical for eternity (Einstein 1930), whereas the Big Bang model describes an evolutionary Universe with finite time.

This behavior was predicted by the de Sitter effect based on Einstein's Theory of General Relativity (Einstein 1920)

¹ Later it was discovered, that distances to galaxies were underestimated by a factor of 2. This was so because Cepheid calibrations were conducted indistinctly for stars belonging to Population I and II, which indicates their age. However, different populations of stars have different metallicity and hence different magnitudes. It was shown by Walter Baade 1925 that Population I Cepheids were about 1.5 magnitudes brighter (Baade et al. 1925). Therefore, Lemaître's and Hubble's values are much higher than modern calculations.

as indicated by (Hubble 1929). This theory predicts the expansion of the Universe, which means that space-time itself is expanding and carrying the galaxies with it. Therefore, the cosmological redshift may not be interpreted as a relative velocity from us, but as the addition of the peculiar motion of the galaxy and the stretching of the wavelength caused by the expansion of the space along their travel. The motion of galaxies due to the expansion of the Universe is referred to as the Hubble flow, while the specific motions of each galaxy are known as the peculiar motions.

Therefore, the Hubble constant stands for the rate of expansion of the Universe, as described by Einstein's theory. It may deduced that, if the Universe is expanding, it must have been smaller before. And if we imagine the history of the Universe, the only possible conclusion is that at the beginning of time, all of the galaxies and all of the Universe must have converged into a single point, what is called the Big Bang. The time since the Big Bang elapsed is referred to as the Hubble time.

Additionally, we now know that the scale factor of the Universe is described by the Friedmann equations (Friedmann 1924). These are a set of equations that describe the scale factor of the Universe, the scale factor $a(t)$ gives the relative scale of the Universe at any time t in comparison with the scale at another time (Nemiroff et al. 2008). The value of the Hubble constant is fundamental to these equations as it sets the expansion rate of the Universe and hence influences its scale. Further understanding of the Friedmann equations brings to the expression of a Hubble constant that is time-dependent, referred to as the Hubble parameter (Harwit 2006):

$$H(t) \equiv \frac{\dot{a}(t)}{a(t)} \quad (2)$$

This serves as mathematical proof that the Hubble constant may have not remained the same throughout the history of the Universe. And shows that our value of the Hubble constant is only meaningful for our time, hence that measurable Hubble constant is labeled H_0 . Moreover, these equations

relate the Hubble parameter with the deceleration constant q_0 which is another fundamental number to cosmology that sets the acceleration of the expansion of the Universe (Ryden 2017):

$$a(t) = 1 + H_0(t - t_0) - \frac{1}{2}q_0H_0^2(t - t_0)^2 \quad (3)$$

Thus, if we knew the value of the Hubble constant, then we could determine the deceleration constant and the scale factor of the Universe. The consequence would be that we could more profoundly study our model of the Universe, discussing the future of the Big Bang model. This means answering questions like whether the Universe will keep expanding or shrink again like the Big Bang.

Since those first calculations in the early 20th century, the Hubble constant has been determined on numerous occasions with multiple methods, despite that it can not be agreed on the exact value of it. The first method consists of using Standard candles, for example, Cepheid variable stars, Supernovae Type Ia or Red Giant stars e.g. (Freedman et al. 2010). At the beginning of the 2000s, a new method was developed using the Cosmic Microwave Background (CMB) modeling anisotropies in the history of the Universe based on the Λ -CDM model e.g. (Komatsu et al. 2009). At first, both methods provided similar results, however as both techniques have become more precise, now their measurements are diverging. For example, the Hubble Space Telescope Key Project computed a value of $H_0 = 72 \pm 8 \text{ kms}^{-1}\text{Mpc}^{-1}$ (Freedman et al. 2001) using Cepheid variables and Supernovae Ia as standard candles, whereas the most recent CMB measurement by the Planck Space Telescope collaboration computes a value of $H_0 = 67.4 \pm 0.5 \text{ kms}^{-1}\text{Mpc}^{-1}$ (Aghanim et al. 2020).

This problem is known as the "crisis in cosmology" or "Hubble tension" (Di Valentino et al. 2019). Possible discussed solutions to this issue are errors in the measurements, such as an erroneous model of the Universe, Λ -CDM model, (López-Corredoira et al. 2022) or a systematic bias in our methods to measure astronomical distances.

More recently, research on the Hubble Tension is being conducted by combining electromagnetic wave and gravitational wave data by the LIGO collaboration (Abbott et al. 2017). This method has given a value of $H_0 = 70.0^{+12.0}_{-8.0} \text{ kms}^{-1}\text{Mpc}^{-1}$, which agrees with the previous calculations.

In this paper, we recompute the Hubble constant using the standard candles method. In order to do this, we need both the distance to the galaxies and their radial velocities. This paper is organized as follows. In section 2 we discuss the use of Cepheid variable stars as standard candles, we explain our method for computing velocities and indicate the source of the data used. Then, in section 4, we discuss the results and derived value of the Hubble constant, and we relate them to the Big Bang model of the Universe. And finally, we draw a conclusion in section 5.

2 METHODS

For computing the Hubble constant we require two measurements: galaxy distance and their radial velocities. In the following two sections we describe how we computed these values (Hubble 1929).

2.1 Distance measurement

Standard candles are astronomical objects that have a known luminosity and can be used to compute large distances, where direct trigonometric distances (parallax) are not feasible. Cepheid variable stars are one type of standard candles, which we use to compute the distance to other galaxies. Cepheid variables have a pulsating luminosity function, which can be measured in periods with a length in the order of days. A Period-Luminosity relation was established by the astronomer Henrietta Swan Leavitt by comparing the brightness of Cepheids in the Magellanic Clouds to those in globular clusters (Leavitt 1908).

A way to compute the distance to stars would be to use their absolute magnitude, which, for most of the stars we can not measure directly. The advantage of Cepheid variables is that their absolute magnitude can be derived from their variability period, and thus their distance can be derived only using their apparent magnitude, which we can measure easily from Earth. Astronomers have used globular clusters and other dwarf galaxies of our galaxy to calibrate the relation between the period and the absolute magnitude, which is referred to as the Leavitt Law. Modern telescopes have enabled more accurate calibrations for instance Tanvir's calibration (Tanvir 1996), which is the one used in this work:

$$M_V = -2.774(\pm 0.083) [\log(P) - 1.4] - 5.262(\pm 0.040) \quad (4)$$

$$M_I = -3.039(\pm 0.059) [\log(P) - 1.4] - 6.054(\pm 0.028) \quad (5)$$

These equations relate the absolute magnitude (M) in the visual (V) and infrared (I) bands, where P is the measured period in days. Once we have determined the absolute magnitude, and because we see the apparent magnitudes, we can use them to derive the distances. To do so we use the following equation:

$$m - M = 5 \log\left(\frac{d}{10 \text{ pc}}\right) \quad (6)$$

or solving for d :

$$d = 10 \cdot 10^{\frac{m-M}{5}} \quad (7)$$

Here, m is the apparent magnitude in the V or the I band, and d is the distance to the star in parsecs [pc]. This process is repeated for each Cepheid variable of the Galaxy Sample. Then the mean distance of a group of Cepheids that belong to the same host galaxy is computed, which we assume to be the distance to the galaxy itself.

2.2 Radial velocities

Velocities are computed using the Doppler Effect on the spectrum of the observed galaxies. Different chemical elements emit or absorb light at very specific wavelengths of the electromagnetic spectrum. When we look at galaxies we primarily see the light emitted by its stars. By dispersing the galaxy's light with a spectrograph we can analyze the absorption lines and deduce which elements compose the stars it is hosting. Furthermore, when observing objects in movement, these absorption lines are shifted along the spectrum. In our case, this is due to the radial velocity of the galaxy

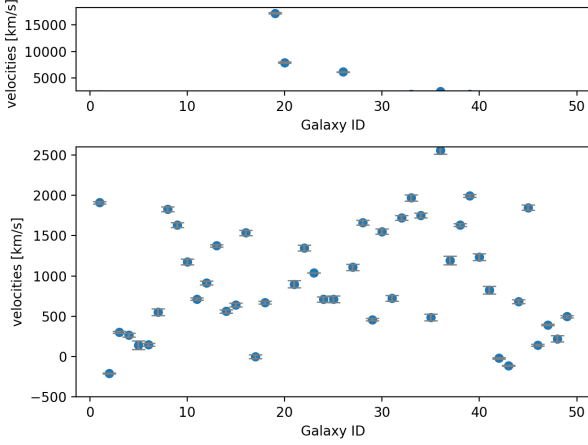


Figure 1. In this diagram the velocity (computed from equation 9) for each galaxy is shown in $[km\,s^{-1}]$. Each galaxy is labelled from 1 to 49 for further comparison with Table 1.

(Humason 1931). By comparing the shift on the spectrum its redshift can be derived with the equation:

$$z = \frac{\lambda_{ob} - \lambda_{em}}{\lambda_{em}} \quad (8)$$

Where λ_{ob} is the observed wavelength and λ_{em} is the emission wavelength of a chemical element. When the object is moving towards us, we get negative redshift, $z < 0$, sometimes also called blueshift. Knowing the redshift of an object we can calculate its radial velocity v as follows:

$$v = c \cdot z \quad (9)$$

Where c is the speed of light, $c = 299\,792\,458\,ms^{-1}$.

3 OBSERVATIONAL DATA

We have used the data from the Extragalactic Cepheid database (ECD)², which includes the periods and apparent magnitudes in V and I bands for each Cepheid variable. The Galaxy Sample list consists of all galaxies on the ECD with at least 10 Cepheids with available period and magnitude data in both bands. This makes a total of 3935 Cepheid stars for a total 49 galaxies. We have computed the distances following equations 4, 5 and 7.

We have collected redshift data from the NASA IPAC Extragalactic Database (NED)³. And we have computed radial velocities using equation 9.

The results of these calculations, both the distances and the radial velocities, are shown in Table 1.

4 RESULTS AND DISCUSSION

Using the previous data we have computed the radial velocities shown in Figure 1. The error range for velocities is derived from the redshift data error.

The data covers a range from $-0.25 \cdot 10^7\,ms^{-1}$ to $1.75 \cdot 10^7\,ms^{-1}$. However, except for three galaxies (19, 20 and 26),

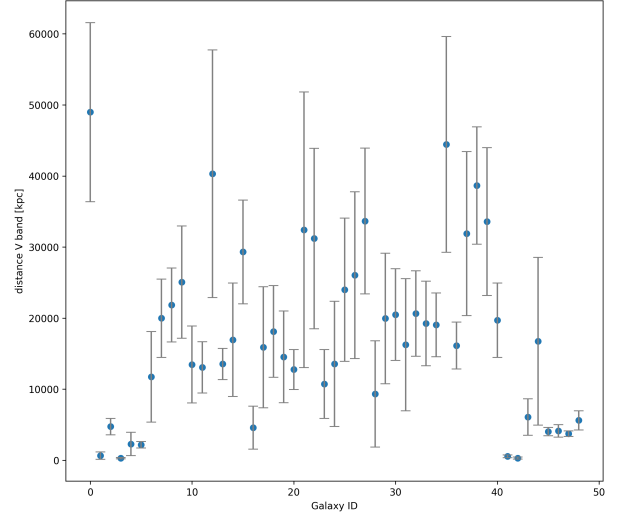


Figure 2. This diagram illustrates the data of the distances from the visual (V) band in $[kpc]$ plotted for each galaxy on the sample. Galaxies are labelled under IDs 1 to 49 and further information about each one can be checked in Table 1. Here it is shown that the range of distances goes from 0 to 50 000 kpc . This data corresponds to the results of equations 4 and 7.

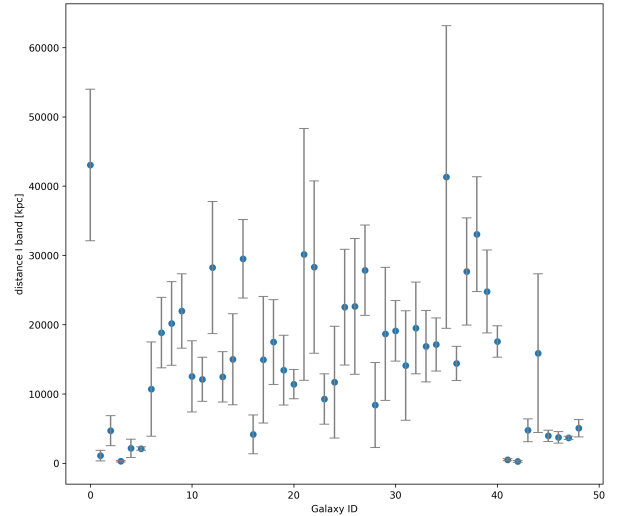


Figure 3. Distances from the Infrared (I) band in $[kpc]$ are plotted for each galaxy on the sample. Galaxies are labelled under IDs 1 to 49 and further information about each one can be checked in Table 1. The range of infrared distances goes from 0 to 50 000 kpc , being in the same range as the visual distances. This data was gathered from the results of equations 5 and 7.

the majority of velocities are found under $0.26 \cdot 10^7\,ms^{-1}$. It also stands out that four galaxies (2, 17, 42 and 43) present negative velocity, meaning they are moving towards us.

Results for the distance calculations explained in section 2.1 can be seen in Figure 2 and 3. We have computed the distance in V band and I band for each galaxy, and the average of both bands stands for the final distance to the galaxy. These final distances are collected in Table 1.

To derive the Hubble constant distances are plotted against their radial velocities, the Hubble constant is the

² <https://cepheids.konkoly.hu>

³ <https://ned.ipac.caltech.edu/>

ID	Galaxy	Membership	Nº of Cepheids	Distance [kpc]	redshift	Radial Velocity [kms ⁻¹]
1	DDO 193	-	32	46012±106	0.0063660	1908.4
2	DDO 008	Local Group	91	863±131	-0.000685	-205.4
3	IC 4182	Canes Venatici I Group	27	4713±175	0.0010086	302.4
4	DDO 74	Local Group	56	287±635	0.000890118	266.9
5	NGC 0055	Local Group	135	2213±355	0.00047948	143.7
6	NGC 0300	Sculptor Group	16	2137±1477	0.000493087	147.8
7	NGC 0925	NGC 925 Group	111	11213±305	0.001839545	551.5
8	NGC 1326A	Fornax Group	19	19412±697	0.006093875	1826.9
9	NGC 1365	Fornax Group	52	21008±862	0.0054445	1632.2
10	NGC 1448	NGC 1433 Group	89	23515±2905	0.00391812	1174.6
11	NGC 1637	field galaxy	41	12992±1663	0.002383862	714.7
12	NGC 2090	field galaxy	34	12588±1295	0.003052556	915.1
13	NGC 2442	-	433	34281±2108	0.0045829	1373.9
14	NGC 2541	NGC 2841 Group	28	13005±6809	0.001873885	561.8
15	NGC 2841	NGC 2841 Group	23	15976±4231	0.002136171	640.4
16	NGC 3021	-	31	29412±6587	0.005119852	1534.9
17	NGC 3031	M81 Group	158	4368±2455	-1.11538E-06	-0.3
18	NGC 3198	NGC 3198 Group	70	15417±3399	0.00223803	670.9
19	NGC 3319	NGC 3198 Group	31	17803±5273	0.057366138	17197.9
20	NGC 3351	Leo Group	49	13986±8446	0.026526711	7952.5
21	NGC 3368	Leo Group	19	12085±2908	0.002993286	897.4
22	NGC 3370	LGG 219	199	31283±5745	0.004488	1345.5
23	NGC 3447	LGG 225	127	29747±8825	0.003474	1041.5
24	NGC 3621	field galaxy	69	9988±2879	0.002370042	710.5
25	NGC 3627	Leo Group	94	12621±8599	0.002371979	711.1
26	NGC 3972	LGG 241	79	23254±11626	0.020627724	6184.0
27	NGC 3982	Ursa Maior Group	58	24346±7279	0.003697511	1108.5
28	NGC 4038	LGG 263	32	30749±6280	0.005539958	1660.8
29	NGC 4258	Canes Venatici II Group	643	8860±4155	0.001535898	460.5
30	NGC 4321	Virgo Cluster	69	19304±5544	0.005175922	1551.7
31	NGC 4414	NGC 4631 Group	11	19788±3755	0.002413563	723.6
32	NGC 4527	Virgo Cluster	64	15171±9399	0.0057465	1722.8
33	NGC 4535	Virgo Cluster	50	20082±5306	0.006564861	1968.1
34	NGC 4536	-	49	18057±5408	0.005838256	1750.3
35	NGC 4548	Virgo Cluster	124	18086±6322	0.001623321	486.7
36	NGC 4603	Centaurus Cluster	61	42881±5608	0.008526125	2556.1
37	NGC 4725	Coma II Group	20	15260±9217	0.003976139	1192.0
38	NGC 5584	Virgo III Cloud	199	29788±6630	0.005448075	1633.3
39	NGC 5917	-	15	35853±10766	0.006645	1992.1
40	NGC 7250	-	29	29180±6491	0.00412615	1237.0
41	NGC 7331	NGC 7331 Group	13	18625±12577	0.002748614	824.0
42	Phoenix dwarf	Local Group	19	520±9637	-6.53636E-05	-19.6
43	DDO 221	Local Group	60	281±18782	-0.000368667	-110.5
44	NGC 5128	Centaurus A Group	56	5418±8187	0.0022722	681.2
45	NGC 4496A	Virgo Cluster	190	16308±8395	0.006164143	1848.0
46	NGC 247	Sculptor Group	23	3987±8269	0.000477615	143.2
47	NGC 5253	M83 Group	13	3924±13487	0.001315483	394.4
48	NGC 7793	Sculptor Group	14	3688±18520	0.000742613	222.6
49	NGC 5236	M83 Group	10	5329±11768	0.001657537	496.9

Table 1. This table collects data of all galaxies in the sample, labelled under the IDs 1 to 49 for comparison with other figures. Names, memberships and the number of Cepheids data were gathered from the ECD database 2, the number of Cepheids column is the sum of Cepheids from which data about the period and apparent magnitudes were available at the time of writing of this paper, i.e. 25 November 2023. The distances column is the average of the distances in V and I bands for the Cepheids of each galaxy, which we assume to be the distance to the galaxy itself. Redshift data was extracted from the NED Database 3, the velocities shown here are computed following section 2 and are also shown in Figure 1.

slope of the linear model that best fits the sets of data, as expressed by Hubble’s Law (equation 1). This equation describes a relation between distance and radial velocities and shows that one could compute the distance to an extra-galactic object only knowing its redshift, and hence the radial velocity, along with the Hubble constant. Thus, the redshift becomes a variable that can be used to measure dis-

tance, provided that we know the exact value for the Hubble constant.

In Figure 4 distances to galaxies are plotted on the x-axis and their radial velocities on the y-axis. To derive the Hubble constant we need to compute the best fit linear regression to these sets of data.

The value of the Hubble constant is the slope, or derivative, of this linear function. Using the full set of points we

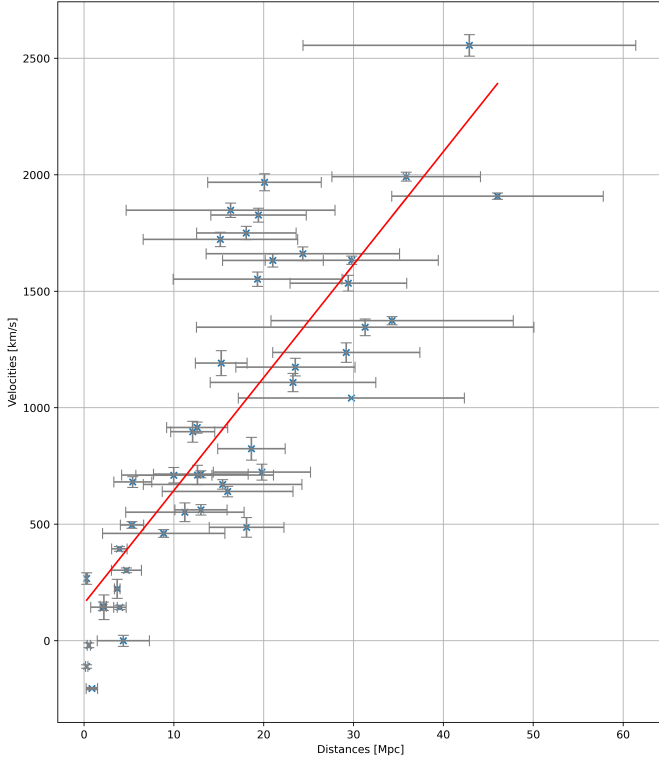


Figure 4. Distance in [Mpc] to each galaxy against their respective radial velocities [km s^{-1}]. The best fit linear regression for the data is illustrated in red. The slope of this linear regression represents the Hubble constant, which we estimated to be $H_0 = 48.5 \pm 5.4 \text{ km s}^{-1} \text{ Mpc}^{-1}$. For this plot we use 46 galaxy data, excluding the 3 of them with outlier data.

compute a value of $H_0 = 54.1 \pm 16.6 \text{ km s}^{-1} \text{ Mpc}^{-1}$. However, we see three galaxies that are evidently outside the linear fit (NGC 3319, NGC 3351 and NGC 3972). If we compute the Hubble constant excluding these three points, we recover a value for the Hubble constant being $48.5 \pm 5.4 \text{ km s}^{-1} \text{ Mpc}^{-1}$.

To compute the measurement uncertainty, we calculate the residuals between the best fit model predictions and the data, taking into account the distance error for each galaxy. Then we compute the Mean Squared Error (MSE) of the weighted residuals and the variance of the distance values. Finally, we calculate the standard error of the slope (MSE / variance).

We observe that the vast majority of galaxies show a positive redshift value ($z > 0$), this means that the majority of galaxies are moving away from the Milky Way Galaxy. This can be explained by a homogeneous and isotropic expansion of the Universe.

Homogeneous means that it is expanding at the same rate in all places, predicting that a galaxy at a distance d will move away at a velocity of dH_0 , while a galaxy at the double distance $2d$, will move away two times faster $2dH_0$. Isotropic means that the expansion is identical in all directions. Because of that, we expect to observe the same from all places in all directions.

It should be taken into account that some galaxies present negative redshift, which are the nearest and may influence the final value of the constant. These are caused when the peculiar motions of one galaxy in the opposite di-

rection of the expansion of the Universe (towards us) are bigger than the velocity of the expansion. These peculiar motions are mainly due to the gravitational interactions between these galaxies. It has been observed that galaxies in the local group are being gravitational pulled towards the Great Attractor (Bertschinger et al. 1988). Gravitational interactions between galaxies and other peculiar motions influence the final result of the Hubble constant. Thus the more galaxies we use, the more accurate the result is.

Deriving the velocities from the galaxy's redshift gives us information about the velocity at which that object is moving towards or away from us along the line of sight. Still, it does not provide information about motion in other dimensions, hence these velocities are being interpreted as radial velocities and thus can be related to the expansion of the Universe.

In comparison with the previous estimates, we can say that our value is not consistent with the measurements mentioned in the introduction, as our value falls below the error margins of both computations (Freedman et al. 2001) and Aghanim et al. (2020). This could be caused by the size of the sample, which considers only 46 galaxies. In addition, we could have used a much modern period-luminosity calibration e.g. (Lazovik et al. 2020) for the distance computations and we could combine different band data to derive much accurate distance values. Besides that, it is interesting to highlight that our measurement is more near to the CMB value (Aghanim et al. 2020) than to the HST Key Project value, which computed their results using Cepheids as standard candles as well as other astronomical objects. This comparison may be illustrated in Figure 5.

Using the value that we just derived for the Hubble constant, we may estimate the time since the Big Band elapsed (Carroll et al. 2017):

$$d = vt = H_0 dt \quad (10)$$

Here, t is the Hubble Time, assuming that the velocity (v), hence the Hubble constant, has remained constant through the history of the Universe. Thereupon, the Hubble time is:

$$t = \frac{1}{H_0} = 20.6125 \pm 2.0597 \text{ Gyr} \quad (11)$$

However, we know that this value is not correct, as the Hubble Time has been evolving with time since the beginning of the Universe.

5 CONCLUSIONS

We have used observational data of redshift from NED (3) database for velocities and data of apparent magnitude and period from ECD (2) database for distance, which we have computed using Cepheid period-luminosity relations. We find a value of $48.5 \pm 5.4 \text{ km s}^{-1} \text{ Mpc}^{-1}$ for the Hubble constant, obtained from a linear fit to the velocity-distance plot of 46 galaxies (Figure 4).

Our value is not in agreement with recent studies as it is below the error range of the measurements mentioned earlier. This could be caused by the distance measurement method we use, as it depends on an empiric calibration. Also, we do not consider additional corrections like interstellar extinction or metallicity of Cepheids, what could impact the

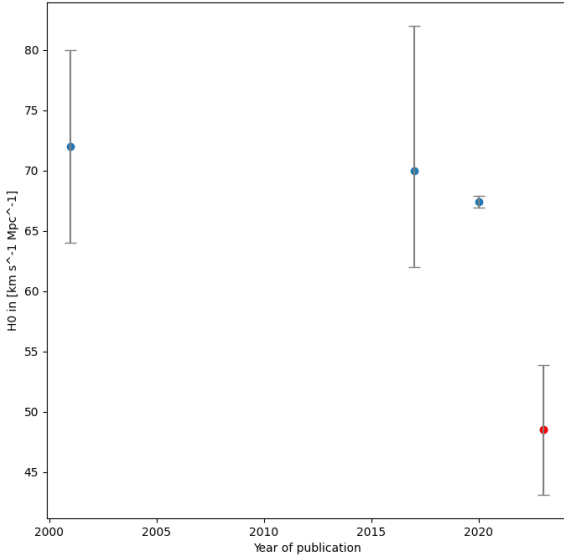


Figure 5. Here it can be seen the relation between estimates of the Hubble constant mentioned in this paper. Our value lays below all previous measurements:

2001: Standard candles, Hubble Space Telescope Key Project
 2017: Gravitational wave, LIGO collaboration
 2020: CMB, Planck
 2023: Standard candles, this paper

distance results. And we use Cepheid as standard candles for the distance computations, which only enables us to use the nearest galaxies and deprives us of including more distant ones. As well, we have not taken into account the velocity error range for computing our value for the Hubble constant.

To achieve higher accuracy in the results more bands could be used and combined, and observational corrections could be taken into account. Using the velocity error range for computing the uncertainty would provide a more precise value. Also, new photometric calibration with larger Cepheid sample could provide a more precise results for distance measurement. In addition, more types of standard candles could be used to prevent bias in the final result due to systematic error in Cepheid period-luminosity relations.

ACKNOWLEDGEMENTS

I would like to thank Ignasi Pérez-Ràfols and Laia Casamiquela for advising this paper and for their helpful support throughout the research. I would also like to thank *Fundació Catalunya La Pedrera* for allowing me to participate in the three-year-long *Youth and Science* program, which has introduced me to scientific research and has led me to the writing of this paper.

References

- ABBOTT B P, ABBOTT R, ABBOTT T D, et al. 2017. A gravitational-wave standard siren measurement of the hubble constant[J/OL]. *Nature*, 551(7678): 85–88. DOI: [10.1038/nature24471](https://doi.org/10.1038/nature24471).
- AGHANIM N, AKRAMI Y, ASHDOWN M, et al. 2020. Planck2018 results: Vi. cosmological parameters[J/OL]. *Astronomy & Astrophysics*, 641: A6. DOI: [10.1051/0004-6361/201833910](https://doi.org/10.1051/0004-6361/201833910).
- Baade W, Malmquist K G. 1925. Die Verwendung der SEARESschen Methode zur Bestimmung des Farbenindex (eposure ratio) fuer Durchmusterungszwecke[J/OL]. *Mitteilungen der Hamburger Sternwarte in Bergedorf*, 5: 2.135-2.147. <https://ui.adsabs.harvard.edu/abs/1925MiHam...5B.135B>.
- Bertschinger E, Juszkievicz R. 1988. Searching for the great attractor[J/OL]. *ApJ*, 334: L59. DOI: [10.1086/185312](https://doi.org/10.1086/185312).
- CARROLL B W, OSTLIE D A. 2017. An introduction to modern astrophysics[M/OL]. Cambridge University Press. DOI: [10.1017/9781108380980](https://doi.org/10.1017/9781108380980).
- DE SITTER W. 1930. On the distances and radial velocities of extra-galactic nebulae, and the explanation of the latter by the relativity theory of inertia[J/OL]. *Proceedings of the National Academy of Sciences*, 16(7): 474-488. DOI: [10.1073/pnas.16.7.474](https://doi.org/10.1073/pnas.16.7.474).
- DI VALENTINO E, MELCHIORRI A, SILK J. 2019. Planck evidence for a closed universe and a possible crisis for cosmology[J/OL]. *Nature Astronomy*, 4(2): 196–203. DOI: [10.1038/s41550-019-0906-9](https://doi.org/10.1038/s41550-019-0906-9).
- EINSTEIN A. 1920. Über die spezielle und die allgemeine relativitätstheorie[M/OL]. Springer Berlin. DOI: [10.1007/978-3-540-87777-6](https://doi.org/10.1007/978-3-540-87777-6).
- EINSTEIN A. 1930. Zum kosmologischen problem der allgemeinen relativitätstheorie[J/OL]. *Verlag der Königlich-Preussischen Akademie der Wissenschaften*: 235-237. <http://echo.mpiwg-berlin.mpg.de/MPIWG:WY9B33EB>.
- FREEDMAN W L, MADORE B F. 2010. The hubble constant [J/OL]. *Annual Review of Astronomy and Astrophysics*, 48: 673-710. DOI: [10.1146/annurev-astro-082708-101829](https://doi.org/10.1146/annurev-astro-082708-101829).
- FREEDMAN W L, MADORE B F, GIBSON B K, et al. 2001. Final results from the Hubble Space Telescope key project to measure the Hubble Constant*[J/OL]. *The Astrophysical Journal*, 553(1): 47. DOI: [10.1086/320638](https://doi.org/10.1086/320638).
- FRIEDMANN A. 1924. Über die möglichkeit einer welt mit konstanter negativer krümmung des raumes[J/OL]. *Zeitschrift für Physik*, 21. DOI: [10.1007/BF01328280](https://doi.org/10.1007/BF01328280).
- HARWIT M. 2006. *Astrophysical concepts*[M/OL]. Springer Science & Business Media. DOI: [10.1007/978-0-387-33228-4](https://doi.org/10.1007/978-0-387-33228-4).
- HUBBLE E. 1929. A relation between distance and radial velocity among extra-galactic nebulae[J/OL]. *Proceedings of the National Academy of Sciences of the United States of America*, 15. DOI: [10.1073/pnas.15.3.168](https://doi.org/10.1073/pnas.15.3.168).
- Humason M L. 1931. Apparent Velocity-Shifts in the Spectra of Faint Nebulae[J/OL]. *ApJ*, 74: 35. DOI: [10.1086/143287](https://doi.org/10.1086/143287).
- KOMATSU E, DUNKLEY J, NOLTA M, et al. 2009. Five-year wilkinson microwave anisotropy probe* observations: Cosmological interpretation[J/OL]. *The Astrophysical Journal Supplement Series*, 180(2): 330. DOI: [10.1088/0067-0049/180/2/330](https://doi.org/10.1088/0067-0049/180/2/330).
- LAZOVIK Y A, RASTORGUEV A S. 2020. Calibrating the galactic cepheid period-luminosity relation from the maximum-likelihood technique[J/OL]. *The Astronomical Journal*, 160(3): 136. DOI: [10.3847/1538-3881/aba627](https://doi.org/10.3847/1538-3881/aba627).
- LEAVITT H S. 1908. 1777 variables in the magellanic clouds [J/OL]. *Annals of Harvard College Observatory*, 60(4): 87-103. <https://nrs.lib.harvard.edu/urn-3:fhcl:2248382>.
- LEMAÎTRE G. 1927. Un univers homogène de masse constante et de rayon croissant rendant compte de la vitesse radiale

- des nébuleuses extra-galactiques[J/OL]. Annales de la Société Scientifique de Bruxelles, A47, p 49-59, 47: 49-59. <https://articles.adsabs.harvard.edu/pdf/1927ASSB...47...49L>.
- LÓPEZ-CORREDOIRA M, MARMET L. 2022. Alternative ideas in cosmology[J/OL]. International Journal of Modern Physics D, 31(08). DOI: [10.1142/s0218271822300142](https://doi.org/10.1142/s0218271822300142).
- NEMIROFF R J, PATLA B. 2008. Adventures in friedmann cosmology: A detailed expansion of the cosmological friedmann equations[J/OL]. American Journal of Physics, 76(3): 265–276. DOI: [10.1119/1.2830536](https://doi.org/10.1119/1.2830536).
- RYDEN B. 2017. Introduction to cosmology[M/OL]. Cambridge University Press. DOI: [10.1017/9781316651087](https://doi.org/10.1017/9781316651087).
- TANVIR N R. 1996. Cepheids as distance indicators[A/OL]. <https://arxiv.org/abs/astro-ph/9611027>.